Available online at www.sciencedirect.com

ScienceDirect

Procedia Manufacturing 54 (2021) 250–256

Procedia MANUFACTURING

www.elsevier.com/locate/procedia

10th CIRP Sponsored Conference on Digital Enterprise Technologies (DET 2021) – Digital Technologies as Enablers of Industrial Competitiveness and Sustainability

Application of the STRAY statistical learning algorithm for the evaluation of in-situ process monitoring data during L-PBF additive manufacturing.

Aoife C. Doyle[a]*, Darragh S. Egan[a], Caitríona M. Ryan[b], Andrew C. Parnell[b], Denis P. Dowling[a]

[a]*I-Form Advanced Manufacturing Research Centre, University College Dublin, Belfield, Dublin. 4, Ireland.*
[b]*Hamilton Institute, I Form Centre for Advanced Manufacturing, Maynooth University, Kildare, Ireland.*

* Corresponding author. Tel.: +353 1 716 2966; *E-mail address:* aoife.doyle1@ucd.ie

Abstract

This study investigates the use of a statistical anomaly detection method to analyse in-situ process monitoring data obtained during the Laser-Powder Bed Fusion of Ti-6Al-4V parts. The printing study was carried out on a Renishaw 500M Laser-Powder Bed Fusion system. A photodiode-based system called InfiniAM was used to monitor the melt-pool emissions along with the operational behaviour of the laser during the build process. The analysis of the in-process data was carried out using an unsupervised machine learning approach called the Search and TRace AnomalY algorithm. The ability to detect defects during the manufacturing of metal alloy parts was demonstrated.

Keywords: Defect detection; In-situ process monitoring; Powder bed fusion; Statistical anomaly detection; High dimensional data; Additive manufacturing;

1. Introduction

Laser Powder Bed Fusion (L-PBF) is an additive manufacturing (AM) technique which fabricates metal parts on a layer-by-layer basis. This process can allow for the creation of complex structures which could not otherwise be fabricated using traditional manufacturing methods [1]. Ti-6Al-4V is a widely used alloy in L-PBF for both the medical device and aerospace sectors due to its superior material properties, including corrosion resistance and resistance to fatigue loading [2][3][5]. Lattice structures, a type of cellular structure composed of non-stochastic in-fill and a high volume of open pores, are an example of complex shaped metallic parts that are producible through L-PBF [6][7]. Despite the many advantages of L-PBF, concerns around the consistency of parts produced have partially limited the wider adoption of this manufacturing method for mission-critical components and necessitate the need for significant post-build quality control checks [8]. Defects occurring during L-PBF include porosity, crack initiation, and/or geometric distortion [9].

The post-build quality control processes currently used in industry face limitations of cost and time [10]. As defects may form at any layer during L-PBF and become permanently sealed in by subsequent layers, a build must be completed before defects and sub-standard mechanical properties can be identified by destructive/non-destructive testing procedures [9][10][11]. To overcome the limitations of post-build checks, in-situ process monitoring (PM) data of the L-PBF process can be utilised for in-situ quality control to identify defective parts as they are being built [10].

In-situ PM is becoming increasingly applied in advanced manufacturing processes [12]. Data can be attained by use of in-situ sensors or by capturing images of the powder bed layer [10][11]. A routine difficulty with data obtained from L-PBF

10.1016/j.promfg.2021.07.039

processes is that it often contains a considerable level of 'noise', or random variation in the signal.

Methods of noise reduction for such processes include the use of digital filters to smoothen signals. One such approach is the use of a Savitzky-Golay filter to calculate smoothed signal values from local polynomial regression [13]. A linear least squares method is used to fit the polynomial in the time domain. This technique has been demonstrated to remove noise from acoustic emission data coming from a Directed Energy Deposition AM process [13]. For the Savitzky-Golay filter, the parameters are the filter order and filter length. Another method for smoothing AM signals is a low-pass Butterworth filter, which has previously been used on the pyrometry data of an L-PBF process obtained during the printing of stainless steel [14]. When employing this filter, a cut-off frequency value is used to determine which frequencies of the signal remain unchanged, and which frequencies are attenuated [15]. The order of the filter also affects its behaviour, where an increase in order improves the rate of attenuation after the cut-off frequency. The method of Moving Average smoothing has been used on L-PBF data obtained during the printing of a Ti-6Al-4V lattice structure [16]. This filter operates by averaging multiple points in a recursive fashion and is applicable to signals in the time domain. Additionally, noise removal has been achieved using a Gaussian filter on L-PBF powder bed images [17]. This was performed by convolving the images with a matrix of numbers that represents the shape of a Gaussian 'bell-curve'. Gaussian smoothing of in-situ PM signal data can be achieved by multiplying the signal by a Gaussian window function, where the product is zero-valued outside of the interval determined by a Gaussian function [18]. The window size controls the number of data-points to be isolated and filtered.

Sophisticated statistical methodologies are required in order to harness the capability of in-situ PM data to detect anomalies during production, improve performance and efficiency and provide decision support for machine operators. In statistics, anomaly detection is concerned with identifying atypical behaviours of a system. Anomaly detection has two main, conflicting objectives: One downgrades the value of anomalies and attempts to eliminate them, while the other demands special attention be paid to anomalies and root-cause analysis be conducted [19][20][21]. Reviews of anomaly detection methods using statistics, machine learning, and experimental studies can be found in [22][23][24].

This article evaluates a newly published unsupervised machine learning approach called the Search and TRace AnomalY (STRAY) algorithm for the evaluation of in-situ PM data obtained during the L-PBF of lattice structures. STRAY uses the k-nearest neighbour (knn) distances between data-points to calculate an anomalous score, and then implements extreme value theory to determine an anomalous threshold from these scores [20]. The algorithm works by first normalizing the recorded data for a single attribute/variable to eliminate the effects of large variance in observations on the nearest neighbour distances. STRAY then calculates the knn distances for all datapoints and orders the successive differences between knn distances. The largest difference between each datapoint's successive knn distances is deemed its 'anomalous score'. The anomalous threshold calculation begins from a subset of 50% of the points with the lowest anomalous scores, under the assumption that this subset contains the anomalous scores corresponding to typical data points and that the remaining subset contains scores corresponding to possible anomalies. Following the Weissman spacing theorem from extreme value theory, an exponential distribution is applied to the upper tail of anomalous scores in the first subset, and an anomalous threshold for the next anomalous score is calculated from a fitted cumulative distribution function. The lowest anomalous score is chosen from the second subset, which is used to either flag all the other points in the subset as anomalies if the score exceeds the threshold or is otherwise declared typical and added to the first subset, where the threshold is updated.

Amongst the advantages of STRAY, is its versatility. For example, it can be applied to one dimensional data for univariate analysis, where the dataset has a single attribute, as well as high-dimensional data for multivariate analysis, where the dataset contains multiple attributes. STRAY has been successfully applied to high-dimensional datasets; however, it has not previously been applied to process monitoring data obtained from manufacturing operations.

In this study, the capabilities of the STRAY algorithm for anomaly detection of in-situ PM data have been assessed using F1-scores. The F1-score is an assessment of predictive model accuracy, which is calculated from the precision and recall values of the model. While an increase in the precision of a predictive model decreases its recall capability, the two metrics can be optimally blended using their harmonic mean, the F1-score, which is widely used to measure the success of a binary classifier when one class is rare [25].

2. Creation of lattice structures

Ti-6Al-4V lattice structures were created using a Renishaw 500M L-PBF system. This system utilises a 500 W laser (λ = 1.07 μm), with a focused spot size diameter of approximately 80 μm. All test pieces were fabricated using Ti-6Al-4V grade 23 powder, obtained from AP & C, with powder particle diameters in the range of 15–45 μm. Prior to the build commencing, a vacuum was used to remove the level of oxygen in the chamber. Following this, argon gas was introduced to achieve an inert atmosphere. The build platform was maintained at a temperature of 170 °C. During the build, a photodiode based in-situ process monitoring system called InfiniAM was used to provide feedback on the laser energy input, known as the Beam Dump (BD) signal [16]. The system employs a further two photodiodes to monitor the emissions emitted from the melt-pool during the melting process, known as photodiode 1 (PD1) and photodiode 2 (PD2). These melt-pool monitoring photodiodes detect in two different wavelength ranges, providing information relating to the plasma (PD1) and infrared (IR) (PD2) emissions created during the L-PBF process.

The photodiodes measure the melt-pool emissions in Volts, which the InfiniAM system converts into bits. These measurements can be used to monitor the presence of process defects and by-products on the powder bed, where higher IR

and plasma emissions may be caused by the insulative properties of powder located inside pores/cavities over which the laser scans, and lower emissions may indicate the presence of conductive by-products, such as spatter. The data acquired by the InfiniAM system is considered high dimensional, as a measurement from all three sensors is captured at an acquisition-rate of 100 kHz. For every layer of data generated, the mean of each photodiode was found, and these values were used for analysis.

The lattice test specimens consist of a 15 × 15 × 28 mm lattice structure, composed of 1.5 mm diamond unit cells and were created using an exposure time and laser power of 750 µs and 150 W respectively, at a layer height of 30 µm. Control samples were printed using these parameters throughout the entire structure, while the other test samples were created containing layers with reduced input laser power to assess anomaly detection capabilities. It would be expected that greater reductions in power would lead to layers being more accurately identified as anomalous, due to the greater contrast in sensor readings between layers built at the typical energy level and layers of reduced energy.

Three batches of lattice specimens were created, each incorporating a number of layers printed with reduced laser power. In the first batch, an energy reduction of 33% was used, referred to as the S1 sample batch. The second and third batch of samples used an energy reduction of 66% and 100%, referred to as S2 and S3 respectively, where the laser did not fire during the selected layers of the S3 batch. The number of layers with reduced laser energy was varied between 1, 3, 5, 7 and 9. The reduction in laser energy occurred between layers 613 and 621, as shown in Figure 1. In this text, samples have a notation of SxVy, where x indicates the level of energy reduction and y indicates the number of affected layers. For example, S1V3 corresponds to a 33% reduction for 3 layers of the build. Note that samples S3V5, S3V7 and S3V9 were excluded from the study as the parts could not be built due to the high number of layers with no input energy. The sample size for each specimen type was n = 4, where the samples were printed close to the four corners of the build-plate to account for emission variations due to build-plate location. The notation associated with each test sample can be viewed in Table 1.

Table 1: Notation associated with each test sample produced in this study, where the S value indicates the level of reduction in laser power for the number of layers given by the V value. Note that samples marked with * were excluded from the study as the parts could not be built due to the high number of layers with no input energy.

No. of layers	Reduction in laser power		
	33%	66%	100%
1	S1V1	S2V1	S3V1
3	S1V3	S2V3	S3V3
5	S1V5	S2V5	S3V5*
7	S1V7	S2V7	S3V7*
9	S1V9	S2V9	S3V9*

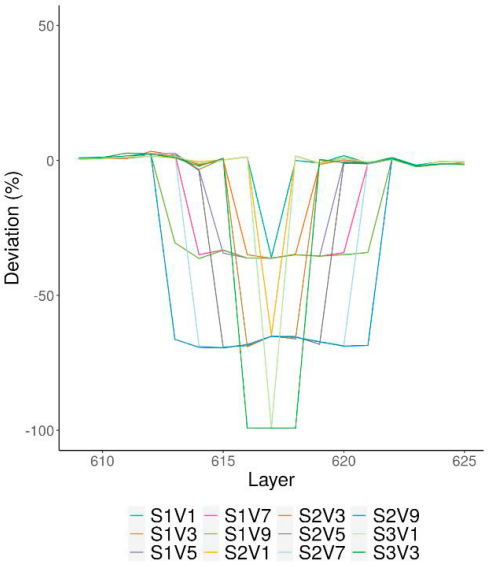

Figure 1: Effect of energy reduction level and the number of affected layers on the deviation between the data obtained from a control build and that from the reduced energy build, displayed in the BD signal.

Fig. 2. An unintentional defect present in a lattice structure due to a wiper tear.

During the build process, a designed control sample was subject to interference from wiper damage, which resulted in the formation of a gross defect with a diameter of approx. 2 mm, as seen in Figure 2. The in-situ PM data corresponding to this lattice structure was examined as an example of a defect occurring at the melt-pool.

3. Application of STRAY to L-PBF in-situ process data

During the L-PBF processes, an in-situ monitoring system was utilised to gather melt-pool and laser related data. In-situ PM data was obtained for 752 layers during the printing of parts containing intentional defects based on the reduction in energy during the printing of up to 9 layers of the Ti-6Al-4V lattice structures. The mean sensor values of each test specimen were calculated for every layer of the build. The mean sensor values of each layer were compared to the mean sensor values of the control sample data in the same layer, and this deviation from the behavior of the control sample was recorded. The sample size for each test was n = 4. The mean deviation values of these

samples were used as an input to the STRAY algorithm. The STRAY algorithm classifies all layers as 'anomalous' or 'typical', depending on whether the anomaly score of the layer exceeds an anomalous threshold that has been calculated from the dataset, using extreme value theory. Data was also obtained from an unintentional defect based on wiper damage during production. The wiper defect, which was outlined earlier, resulted in a 2 mm diameter pore which is approximately located between layers 690 and 757. The mean sensor values of the test specimen were calculated for every layer of the build, and the deviation from the behavior of the control sample was used as an input to the STRAY algorithm.

Univariate and multivariate analyses were conducted on both L-PBF process datasets to assess the capabilities of the STRAY algorithm to detect anomalies using data from a single sensor, or from multiple sensors. The effects of smoothing/filtering techniques were also investigated. The techniques considered in this study were Savitzky–Golay filtering, low-pass Butterworth filtering, Moving Average filtering, and Gaussian filtering. To mitigate the effects of individual filter parameter choices on the results of anomaly detection, anomaly detection was executed at a range of values for each filter parameter. Only the anomalies that were commonly identified at each filter parameter value were recorded. For the Savitzky-Golay filter, the variable parameters were the filter order and filter length. The parameters involved in Butterworth filtering were filter order and cut-off frequency. The window size was the variable parameter used in the Moving Averaging and Gaussian filtering. The range of values for each filtering parameter was chosen through experimentation, and further experimentation is needed for parameter optimisation.

The average F1-scores of the 12 parts built with intentional defects were recorded to assess the capability of the STRAY algorithm to detect anomalies in filtered and unfiltered signals. The capability of the STRAY algorithm to detect anomalies in the filtered and unfiltered data of the specimen with an unintentional defect was visually assessed, as precision and recall values cannot be properly calculated when the exact number of layers affected by the wiper tear is unknown.

4. Results

4.1. Dataset with intentional defects

Univariate analysis of sensor deviation data

For the Beam Dump (BD) univariate analysis of intentionally designed defects, the number of anomalies detected in the unfiltered signal closely matched the designed number of layers with an intentional defect. Most filtering methods resulted in mediocre F1-scores, as can be seen in Table 2, as false positive anomalous layers were present in the Savitzky-Golay, Butterworth and Moving Average signals. For the univariate analysis of PD1 in the dataset of intentionally designed defects, no anomalies were detected in the unfiltered signal. Certain filtering methods also occasionally resulted in instances of no anomalies being detected, leading to false negative results being recorded. The analyses where such instances occurred are denoted by * in Table 2, and the number of instances can be seen in Table 3. An example of anomaly detection in the PD1 signal for part S3V3 can be seen in Figure 3, where there was a 100% input energy reduction over 3 layers. Note that the plot contains overlaid anomalies from each filtering method, which may limit visibility of some anomalies. Similar to PD1, no anomalies were detected in the unfiltered signal during the univariate analysis of PD2. Certain filtering methods occasionally resulted in instances of no anomalies being detected, as shown in Table 3. The Savitzky-Golay and Moving Average are examples of filtering methods which occasionally led to false negatives being recorded, but otherwise contributed towards high F1-scores scores in PD1 and PD2, as detailed in Table 2. The Butterworth filter showed no instances of recording false negatives, but occasionally recorded false positives. The Gaussian filter predominantly resulted in no anomalies being recorded in PD1 and PD2, except for part S3V3 in PD1.

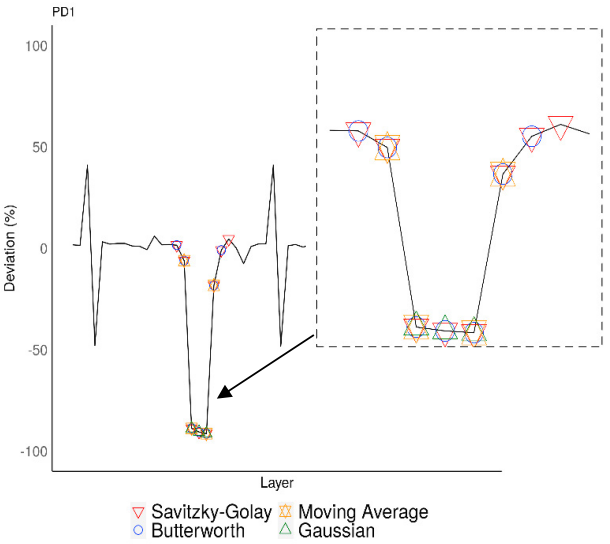

Figure 3: Anomalies identified in the univariate PD1 deviation signal of a part with an intentional defect, where layers 600 – 655 are displayed on the horizontal axis. The colours/shapes indicate the anomalies identified using STRAY with different smoothing techniques.

Table 2: F1-scores of univariate (U.V) and multivariate (M.V) analyses of parts with intentional defects. Analyses where no anomalies have been detected in certain samples are denoted by: *

Method	BD (U.V)	PD1 (U.V)	PD2 (U.V)	M.V
No filter	0.98	-*	-*	1*
Savitzky-Golay	0.38	0.68*	0.74*	0.52*
Butterworth	0.42	0.65	0.58	0.44
Moving Average	0.45	0.84*	0.84*	0.71*
Gaussian	0.82	1*	-*	1*

Table 3: Number of instances where no anomalies have been detected in a sample during univariate (U.V) and multivariate (M.V) analyses of parts with intentional defects.

Method	BD (U.V)	PD1 (U.V)	PD2 (U.V)	M.V
No filter	0	12	12	10
Savitzky-Golay	0	4	4	1
Butterworth	0	0	0	0
Moving Average	0	3	5	1
Gaussian	0	11	12	5

The magnitude increase of signal deviation in PD1 closely mirrors the decrease of input laser energy. This can be seen in Figure 3 where an energy reduction of 100% in sample S3V3 has led to a signal deviation of approximately 91% being recorded in the plasma data for the corresponding layers. This phenomenon is also evident, but less pronounced, in the IR data, with a signal deviation of approximately 78% being recorded over the corresponding layers of the same sample.

Multivariate analysis of sensor deviation data

The results of multivariate analysis for this dataset can be seen in Table 2 and 3. By contrast to the univariate analysis, the unfiltered signal has led to the correct number of anomalies being detected in 2 lattice samples. The Savitzky-Golay and Moving Average methods of smoothing have resulted in a lower number of instances where no anomalies have been detected in a sample than in univariate analysis. Gaussian filtered data resulted in certain instances of false negatives, however, the STRAY algorithm has performed well when using Gaussian filtered data in all samples where the reduction in input energy is greater than 33%.

4.2. Dataset with unintentional defect

The wiper defect resulted in a 2 mm diameter pore, occurring approximately between layers 690 and 757. This experimental observation of a processing defect is valuable, as it provides a dataset which contain both anomalous and normal behaviour generated by the melt-pool sensors. As the anomaly was caused by a wiper tear, the laser input energy data did not change from that obtained for the rest of the lattice sample. Both univariate and multivariate analysis was carried out using STRAY, and the effects of smoothing/filtering techniques were also investigated on this data by executing anomaly detection at a range of values for each filter parameter and recording only the anomalies that were commonly identified at each filter parameter value.

Univariate analysis of sensor deviation data

For the univariate analysis of the BD signal, it is evident from Figure 4 that over identification has occurred, particularly in the unfiltered signal, as no anomalous behaviour should be present in this signal. This is not the case for the PD1 and PD2 photodiode signals, where each identified anomaly is present within the expected range of defective layers. Analysis of the PD1 data has shown that 7 anomalies were identified in the

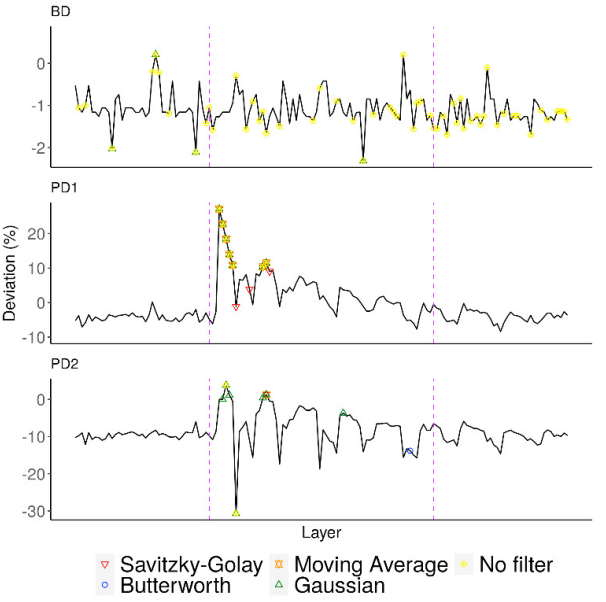

Figure 4: Anomalies identified in the individual signals during univariate analysis of a part with an unintentional defect, where layers 650 –797 are displayed. The vertical, dashed lines indicate the approximate region where the wiper tear has affected the build.

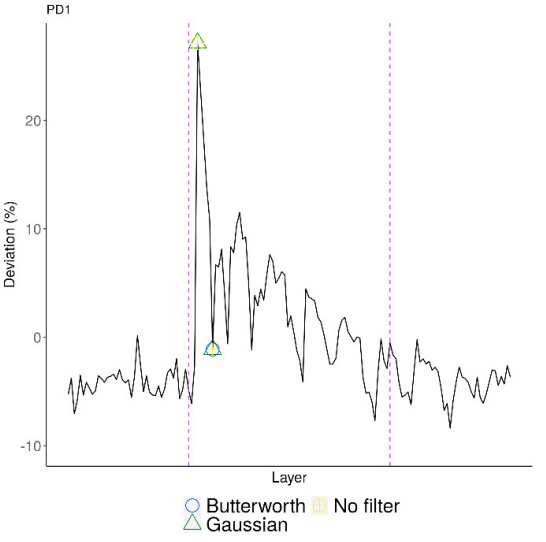

Figure 5: Anomalies identified during multivariate analysis of a part with an un-intentional defect, displayed on the PD1 signal for layers 650 - 797.

unfiltered data. The same number of anomalies has been detected in the Butterworth, Moving Average, and Gaussian filtered signals, while 10 anomalies were identified in the Savitzky-Golay filtered signal. For the analysis of PD2 in this dataset, 2 anomalies were identified by using the unfiltered and Butterworth filtered signals. One anomaly was identified using the Savitzky-Golay and Moving Average filtered signals, and 7 were identified using the Gaussian filtered signal. This result demonstrates that univariate analysis can detect the process defect from the in-situ PM data, while also showing how data filtering can improve analysis, particularly in the BD signal.

Multivariate analysis of sensor deviation data

For multivariate analysis of an unintentionally designed defect, 2 anomalies were identified in the unfiltered signal. No anomalies were identified using the Savitzky-Golay or Moving Average methods of filtering, while the Butterworth and Gaussian methods reported 1 and 2 anomalies, respectively. This result can be seen in Figure 5. This result shows that the multivariate analysis is under-detecting anomalous layers, as approximately 67 layers were affected by the wiper tear during this build. The detected anomalies are present at the most extremely deviated layers where the defect has started to form in the lattice structure.

5. Conclusions

Univariate and multivariate analyses have been conducted on two datasets, one with data from parts containing intentional defects based on the reduction in energy during the printing of Ti-6Al-4V lattice structures, and a second with data from a part containing an unintentional defect due to wiper damage during printing. When performing univariate analysis on the intentional defect dataset, the unfiltered Beam Dump signal demonstrated a high F1-score when identifying the designed defective layers. By contrast, no anomalies were detected in the unfiltered melt-pool signals which is most likely due to the large level of noise which occurs in these signals. The use of filtering techniques improved this analysis. Multivariate analysis of this dataset showed fewer instances where no anomalies were detected, compared with the results obtained using the univariate PD1 and PD2 analyses. Difficulties in detecting anomalies were observed in the case of prints with fewer layers of reduced energy, as well as where the level of energy reduction was smaller.

From analysis of the part containing an unintentional defect, the STRAY algorithm was found to identify multiple false positive anomalies during univariate analysis of the Beam Dump signal, particularly when unfiltered data was used. The most extreme points in the Beam Dump signal data were found to be incorrectly labelled anomalous, due to a lack of contrasting anomalous behaviour. Anomaly detection accuracy is enhanced when the data from PD1 and PD2 was examined, compared with that from the Beam Dump signal, as the wiper tear has affected the photodiode signals. The multivariate analysis results demonstrate how the number of anomalies is greatly reduced for this dataset when taking data from all three sensors into account. This could be caused by the behavioural similarities between PD1 and PD2 resulting in lower anomaly scores being calculated for the wide range of defective layers. The anomalies detected in the multivariate analysis are present at the most extremely deviated layers from the control, where the defect has started to form in the structure.

The use of Savitzky-Golay, Butterworth, Moving Average and Gaussian filtering methods have demonstrated an improvement to the STRAY analysis of noisy signals, where the Savitzky-Golay, Moving Average and Gaussian tend to contribute towards under-detection, and the Butterworth tends to contribute towards over-detection. While these filters were suitable to the L-PBF process, further investigation is needed to determine suitability to other printing methods and materials.

It was observed that the increase in magnitude of melt-pool signal deviation closely mirrors the decrease of input laser energy in the samples containing intentional defects. In the case of the unintentional defect, it is noticeable that the greatest increase in plasma and IR emissions occurs at the beginning of the defect formation, and this deviation decreases as the process corrects itself. This is believed to be a result of the thermal conductivity of the powder, a phenomenon which has been previously investigated by Egan et al. during a study of L-PBF parts being built with designed cavities of various sizes [26]. Due to poor thermal conductivity in the powder bed, the underlying powder in the cavities acted as a thermal insulator when the laser scanned above the defect. As more energy was applied to a given area using the laser, the heat was poorly conducted away from the powder, which resulted in an increased melt-pool size and higher temperature. Higher thermal emissions were, therefore, detected in areas where a cavity was detected by the InfiniAM system. Sudden drops in the InfiniAM IR emissions could be caused by the laser firing onto redeposited spatter, as was hypothesized by Keaveney et al. [27]. This hypothesis is based on the large size of spatter and how it bonds to the previous layer's surface when redeposited, which would conduct the laser's heat into the specimen as opposed to emitting it back out of the melt-pool.

In this study, multivariate analysis took three sensors into account. The STRAY algorithm has the potential to analyse a further number of sensors should they be incorporated into an AM printer, due to its ability to quickly process high-dimensional datasets. This could allow for further sensors to be utilized to maximize the understanding of machine behaviour in typical and anomalous situations.

This study has demonstrated the success of the STRAY algorithm to rapidly process (within seconds) data from 752 layers, obtained using three different photodiodes. By comparison, each layer from the build of Ti-6Al-4V lattice structures took approximately 2 minutes to complete. Due to this speed of processing, this algorithm has the potential to detect anomalies in high-dimensional datasets in real-time.

Acknowledgements

This publication has emanated from research supported in part by a research grant from Science Foundation Ireland (SFI) under Grant Number 16/RC/3872 and is co-funded under the European Regional Development Fund. For the purpose of Open Access, the author has applied a CC BY public copyright license to any Author Accepted Manuscript version arising from this submission'. Andrew Parnell's work was supported by: a Science Foundation Ireland Career Development Award (17/CDA/4695); an SFI Centre for Research Training in Foundations of Data Science 18CRT/6049 award, and SFI Research Centre awards I Form 16/RC/3872 and Insight 12/RC/2289_P2.

References

[1] Slotwinski A, Garboczi EJ, Stutzman PE, Ferraris CF, Watson SS, Peltz MA. Characterization of Metal Powders Used for: Additive Manufacturing. *J Res Natl Inst Stand Techno. Charact* 2014;119:25–29.

[2] Herzog D, Seyda V, Wycisk E, Emmelmann C. Additive manufacturing of metals. *Acta Mater* 2016;117:371–392.

[3] Javaid M, Haleem A. Additive manufacturing applications in medical cases: A literature based review. *Alexandria J Med.* 2018;54:411-422

[4] Santoliquido O, Bianchi G, Dimopoulos Eggenschwiler P, Ortona A. Additive manufacturing of periodic ceramic substrates for automotive catalyst supports. *Int J Appl Ceram Technol* 2017;14:1164–1173.

[5] Shah FA, Snis A, Matic A, Thomsen P, Palmquist A. 3D printed Ti6Al4V implant surface promotes bone maturation and retains a higher density of less aged osteocytes at the boneimplant interface. *Acta Biomater* 2016;30:357-367.

[6] Xiao L, Song W. Additively manufactured functionally graded Ti6Al4V lattice structures with high strength under static and dynamic loading: experiments. *Int J Impact Eng* 2018;111:255–272.

[7] Al Saedi DSJ, Masood SH, Faizan-Ur-Rab M, Alomarah A, Ponnusamy P. Mechanical properties and energy absorption capability of functionally graded F2BCC lattice fabricated by SLM. *Mater Des* 2018;144:32–44.

[8] Lewandowski JJ, and Seifi M. Metal Additive Manufacturing: A Review of Mechanical Properties. *Annu Rev Mater Res* 2016;46:151–186.

[9] Montazeri M, Yavari R, Rao P, Boulware P. In process monitoring of material cross contamination defects in laser powder bed fusion. *J Manuf Sci Eng* 2018;140:111001.

[10] Everton SK, Hirsch M, Stravroulakis P, Leach RK, Clare AT. Review of in situ process monitoring and in situ metrology for metal additive manufacturing. *Mater Des* 2016;95,431–445.

[11] Egan DS, Dowling DP. Correlating in situ process monitoring data with the reduction in load bearing capacity of selective laser melted Ti6Al4V porous biomaterials. *J Mech Behav Biomed Mater* 2020;106:103723.

[12] Grasso M, Colosimo BM. Process defects and in situ monitoring methods in metal powder bed fusion: A review. *Meas Sci Technol* 2017;28:1-25.

[13] Whiting J, Springer A, Sciammarella F. Real time acoustic emission monitoring of powder mass flow rate for directed energy deposition. *Addit Manuf* 2018;23:312–318.

[14] Mahato V, Obeidi MA, Brabazon D, Cunningham P. Detecting voids in 3D printing using melt pool time series data. *J Intell Manuf* 2020:1–8.

[15] Carr J. *The Technician's EMI Handbook.*1st ed. Newnes; 2000.

[16] Egan DS, Ryan CM, Parnell AC, Dowling DP. Using in situ process monitoring data to identify defective layers in Ti6Al4V additively manufactured porous biomaterials. *J Manuf Process* 2021;64,1248–1254.

[17] Scime L, Beuth J. Anomaly detection and classification in a laser powder bed additive manufacturing process using a trained computer vision algorithm. *Addit Manuf* 2018;19:114 - 126.

[18] Prabhu KMM. *Window Functions and Their Applications in Signal Processing*. 1st ed. Boca Raton: CRC Press; 2014.

[19] Abuzaid AH, Hussin AG, Mohamed IB. Detection of outliers in simple circular regression models using the mean circular error statistic. *J Stat Comput Simul* 2013;83,269–277.

[20] Talagala PD, Hyndman RJ, and Smith-Miles K. Anomaly Detection in High Dimensional Data. *J Comput Graph Stat* 2020.

[21] Hodge VJ, Austin J. A survey of outlier detection methodologies. *Artif Intell Rev* 2004;22:85–126.

[22] Lavin A, Ahmad S. Evaluating real time anomaly detection algorithms -- the Numenta anomaly benchmark. *IEEE 14th ICMLA* 2015:38-44.

[23] Chandola V, Banerjee A, Kumar V. Anomaly detection: A survey. *ACM Comput Surv* 2009;41:1-58.

[24] Gupta M, Gao J, Aggarwal CC, Han J. Outlier detection for temporal data: a survey. *IEEE Trans Knowl Data Eng* 2014;26:2250-2267.

[25] Lipton ZC, Elkan C, Naryanaswamy B. Optimal Thresholding of Classifiers to Maximize F1 Measure. In: *Machine Learning and Knowledge Discovery in Databases*, (Calders T, Esposito F, Hüllermeier E, Meo R, editors). Vol. 8725. Berlin, Heidelberg: Springer; 2014.

[26] Egan DS, Dowling DP. Influence of process parameters on the correlation between in-situ process monitoring data and the mechanical properties of Ti-6Al-4V non-stochastic cellular structures, *Addit Manuf* 2019;30:100890.

[27] Keaveney S, Shmeliov A, Nicolosi V, Dowling DP. Investigation of Process By-products during the Selective Laser Melting of Ti6AL4V Powder. *Addit Manuf* 2020;36:101514.